J. Plasma Physics (1999), *vol.* 61, *part* 1, *pp.* 161–168. Printed in the United Kingdom

Excitation of ion acoustic solitons from grids

YASSER EL-ZEIN,[1] T. E. SHERIDAN,[2]
KARL E. LONNGREN[3] and WENDELL HORTON[4]

[1] IBM, East Fishkill Facility, zip 2A1, 1580 Route 52, Hopewell Junction, NY 12533-6531, USA
[2] Plasma Research Laboratory, Research School of Physical Sciences and Engineering, Australian National University, Canberra, ACT 0200, Australia
[3] Department of Electrical and Computer Engineering, and Department of Physics and Astronomy, The University of Iowa, Iowa City, IA 52242, USA
[4] Institute for Fusion Studies, Department of Physics, University of Texas, Austin, TX 78712, USA

(Received 10 August 1998)

Using a particle-in-cell code, we are able to simulate the excitation of ion acoustic solitons from a grid whose potential is suddenly increased. The numerical results are in substantial agreement with previous laboratory experiments.

1. Introduction

A series of laboratory experiments designed to ascertain and specify the requirements that should be imposed on the voltage excitation signal to be applied to planar fine-mesh grid structures inserted in a large quiescent discharge plasma in order to launch ion acoustic solitons has been performed (Lonngren et al. 1982; Gabl and Lonngren 1984). The excitation signal was typically a repetitive low-frequency ($f \approx 1$–10 kHz) square wave with an amplitude $\Delta \approx (1\text{–}5)\,\kappa_B T_e/e$. The optimum rise time of the square wave was $\tau_r \approx (1\text{–}3)/f_{pi}$. Ion acoustic solitons were excited only after the applied voltage signal *switched from a negative to a positive value*. In addition, ions that were either reflected by the soliton or were actually involved in its excitation were detected ahead of it. A dispersing Airy function was launched after the ensuing half-cycle when the polarity switch of the applied signal was in the opposite sequence. The purpose of the present investigation is to numerically simulate the ion acoustic soliton excitation in order to determine the origin and the nature of the ions that were found ahead of the soliton in the experiment. This will allow us to suggest the actual excitation mechanism in this type of experiment.

Numerical codes using a *fluid model* consisting of the nonlinear equations of continuity and motion for the ions, and a Boltzmann assumption for the massless electrons, with the two species coupled together with Poisson's equation, have been developed and widely used to study sheath evolution from electrodes whose potential is suddenly *decreased*. Both two- and three-component plasmas and one- and two-dimensional codes have been developed (Widner et al. 1970; Amin et al. 1993; Hong and Emmert 1994, 1995; Sheridan and Alport 1994; Sheridan 1995; El-Zein et al. 1996). In these studies, it was

found that the electrons are quickly blown into the ambient plasma after the application of a negative-voltage step. A flux of heavy positive ions will be attracted to and absorbed by the electrode, resulting in a rarefactive sheath, which subsequently expands into the background plasma. The flux of impinging ions can alter the surface properties of the electrode, which may have desirable consequences. The sheath expansion is initially faster than the ion acoustic velocity; however, it eventually slows down to this value.

Owing to the assumption of fluid ions, 'collisionless' fluid models cannot adequately describe the case where the electrode potential is suddenly increased, as is the case of interest here. The reason for this is as follows. An increase in the potential on a grid creates an electric field that is largest near the grid and points away from it. Consequently, ions nearer the grid experience a larger acceleration, and may overtake ions that are initially farther from the grid. However, fluid elements cannot simply pass by one another, as do particles – overtaking requires the ion velocity to become multivalued at the position where it occurs. This is not a problem when the electrode is biased negatively, since overtaking does not then occur (for convex electrodes).

We have developed a *particle-in-cell* (*PIC*) code that has been applied to the plasma sheath expansion study described above (Sheridan 1997; Yi et al. 1997b). This code has also recently been used to analyse and interpret ion acoustic soliton excitation from a modulated high-frequency voltage signal whose carrier frequency was greater than the ion plasma frequency (Sheridan et al. 1998). Soliton excitation using this type of applied signal had previously been observed in the laboratory (Yi et al. 1997a; Yi and Lonngren 1997).

In Sec. 2, we briefly summarize the PIC code that was used here and emphasize the features that are unique to the present application. The results and the interpretation of these results are given in Sec. 3. Concluding comments appear in Sec. 4.

2. PIC model

The set of normalized equations we use to model the plasma are as follows.

(i) The equation of motion for the ith ions is

$$M\frac{d^2x_i}{dt^2} = -e\frac{d}{dx}, \tag{1}$$

where M is the ion mass and is the plasma potential.

(ii) The electrons obey a Boltzmann relation

$$n_e = n_0 \exp\left(\frac{e}{\kappa_B T_e}\right). \tag{2}$$

(iii) The electrostatic potential is found by solving Poisson's equation

$$\frac{d^2}{dx^2} = -\frac{e}{\varepsilon_0}(n_i - n_e), \tag{3}$$

where n_i is the ion density.

https://doi.org/10.1017/S002237789800734X Published online by Cambridge University Press

(iv) The left boundary of the simulation box is a partially transparent grid driven with a signal

$$V_{\text{grid}} = \Delta \left[1 - \exp\left(-\frac{t}{\tau_r}\right)\right], \tag{4}$$

where Δ is the amplitude and τ_r is the rise time of the applied signal. Ions passing through the grid and out of the box are reflected back with a probability equal to the transparency of the grid.

The distance is normalized by the electron Debye length, the time is normalized by the ion plasma frequency, the densities are normalized by the background density n_0, the velocities are normalized by the ion acoustic velocity, and the potential is normalized by the electron temperature. The simulations are performed in the region defined by $x > 0$. The right boundary is fixed at $= 0$ and is perfectly absorbing. The initial plasma surrounding the electrode is assumed to be uniform in space, with density $n_e = n_i = n_0$ and electrically charge-neutral. The initial velocity of the ions and the potential are set equal to zero at all positions. The simulation parameters are as follows: simulation grid spacing $= \frac{1}{4}\lambda_D$, number of grid points $= 3072$, time step $\Delta t\omega_{pi} = \frac{1}{32}$, and 64 ion particles initially per cell. With these parameters, the system length is $768\lambda_D$, and there are approximately 200 000 particles in the simulation.

3. Simulation results

The evolution of the plasma close to the electrode at early times after the application of the positive voltage step V_{grid} is shown in Fig. 1. Two values of excitation voltage with a rise time $\tau_r = 0$ are shown. The subsequent propagation of the signals far from the electrode and at later times for the same two excitation signals is shown in Fig. 2. The plasma is initially assumed to be homogeneous, so no steady-state sheath effects are included in our results. We summarize and tabulate the various computed velocities that are normalized by the ion acoustic velocity and perturbed densities normalized by the background density in Table 1.

Ahead of the large pulse, which we shall later identify as a soliton, are two distinct groups of ions. The two groups are most apparent in the trace at $z = 20, V_{\text{grid}} = 20T_e$ in Fig. 1. The velocity of the fastest burst of ions depends on the excitation voltage V_{grid}. We interpret this ion burst as being launched from either a grid or a plate owing to the expulsion of a group of ions that initially are adjacent to but in front of the electrode. These ions gain an energy.

$$\tfrac{1}{2}M_i v^2 = eV_{\text{grid}} \tag{5}$$

due to the electrode's increase in potential. From Table 1, we note that the velocity of the simulated result agrees with this interpretation. This burst of ions interact only weakly with the background plasma due to the large velocity. This ion burst corresponds to the *pseudowave* or a burst of ions that pass through a grid and whose velocity is increased by the increase of the grid potential (Alexeff et al. 1968; Joyce et al. 1969).

The velocity of the second group of ions is approximately twice that of the

https://doi.org/10.1017/S002237789800734X Published online by Cambridge University Press

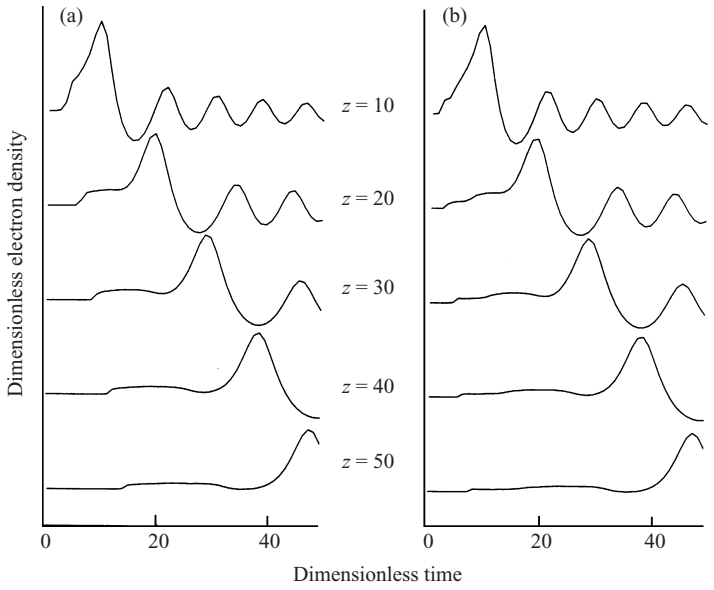

Figure 1. Evolution of the plasma in space and time close to the electrode and at early times for two values of a positive step voltage. The rise time of the voltage step is zero. A voltage-dependent burst of ions, a burst of ions reflected from the soliton, an ion acoustic soliton, and a dispersing ion acoustic wave are sequentially detected. (a) $V_{\text{grid}} = 5T_e$; (b) $V_{\text{grid}} = 20T_e$.

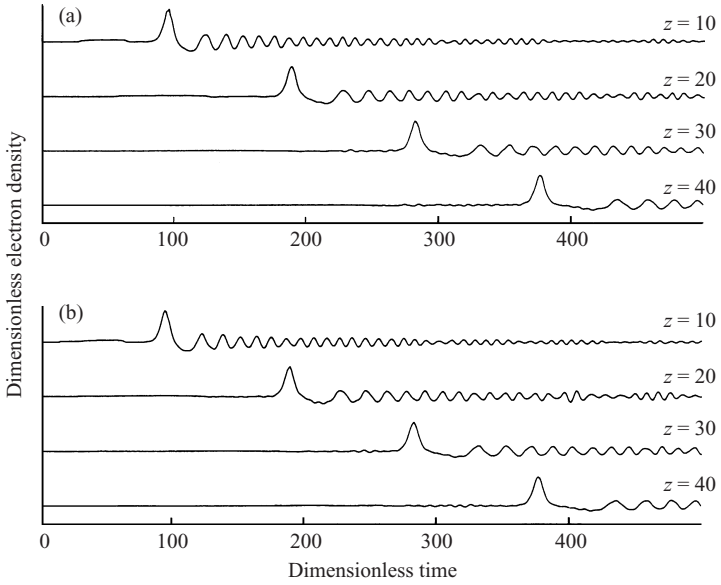

Figure 2. Evolution of the plasma in space and time far from the electrode and at late times for two values of a positive step voltage. The rise time of the voltage step is zero. An ion acoustic soliton and a dispersing ion acoustic wave are sequentially detected. (a) $V_{\text{grid}} = 5T_e$; (b) $V_{\text{grid}} = 20T_e$.

large signal, as noted in Table 1. These ions are reflected from the large propagating positive potential perturbation. We interpret the acceleration mechanism of the ions as being Fermi-accelerated by this moving perturbation (Lonngren et al. 1981).

https://doi.org/10.1017/S002237789800734X Published online by Cambridge University Press

Table 1. Summary of computed velocities normalized by the linear ion acoustic velocity at two values of excitation potential applied to the electrode.

		Simulation				
V_{grid}	$\dfrac{\left(\dfrac{2eV_{\text{grid}}}{M_i}\right)^{1/2}}{\left(\dfrac{\kappa_B T_e}{M_i}\right)^{1/2}}$	Ion burst $\left(\dfrac{\kappa_B T_e}{M_i}\right)^{1/2}$	Reflected ions $\left(\dfrac{\kappa_B T_e}{M_i}\right)^{1/2}$	Soliton $\left(\dfrac{\kappa_B T_e}{M_i}\right)^{1/2}$	$\dfrac{\Delta n}{n}$	$1+\dfrac{\Delta n}{3n}$
$5T_e$	$\sqrt{10} = 3.16$	3.33	2.17	1.09	0.30	1.10
$20T_e$	$\sqrt{40} = 6.32$	6.25	2.17	1.09	0.30	1.10

The largest signal is interpreted to be an ion acoustic soliton, since, as noted in Table 1, its velocity satisfies the Korteweg–de Vries (KdV) velocity requirement that

$$v = \left(\frac{\kappa_B T_e}{M_i}\right)^{1/2}\left(1+\frac{\Delta n}{3n}\right). \tag{6}$$

We note that the velocities of both the soliton and the ions that are reflected ahead of it are independent of the large excitation potential that was applied to the electrode. We shall note later that the soliton amplitude does depend on the excitation potential if it is not large. The soliton separated from the trailing oscillation whose front propagated at the ion acoustic velocity.

In the experiments, it was also noted that the soliton excitation and/or the dispersing Airy function depended upon the rise time τ_r of the applied voltage step (Lonngren et al. 1982; Gabl and Lonngren 1984). In Fig. 3, we present the results of the simulation at two fixed locations ($z = 20$ and $z = 300$). The initial location is close to the electrode, and rise-time effects on the two ion bursts can be followed. As the rise time is increased from zero, the ion burst previously identified as a pseudowave slows down and appears to be absorbed in the reflected ion-soliton signals. This rise-time dependence has also been seen in the laboratory (Lonngren et al. 1970).

At the location $z = 300$, the amplitude of the excited soliton is found to change as the rise time of the applied voltage step is increased. From (6), this amplitude enhancement increases the soliton velocity; hence the increase in separation between the soliton and the trailing linear oscillation is expected. The optimum rise time for soliton excitation is found to be greater than zero – it is in fact a few ion plasma periods.

As a final test to determine if the ions contained in the ion burst identified as the pseudowave strongly interacted with the soliton, we applied an excitation signal that would accelerate ions to be close to the expected soliton velocity. As shown in Fig. 4, at a great distance from the electrode, the excited soliton amplitude does depend upon the exciting signal. The simulated time of flight ΔT for the soliton propagating between the electrode and the point of observation at $z = 600$ agrees with KdV theory for all three signals, as tabulated in Table 2.

https://doi.org/10.1017/S002237789800734X Published online by Cambridge University Press

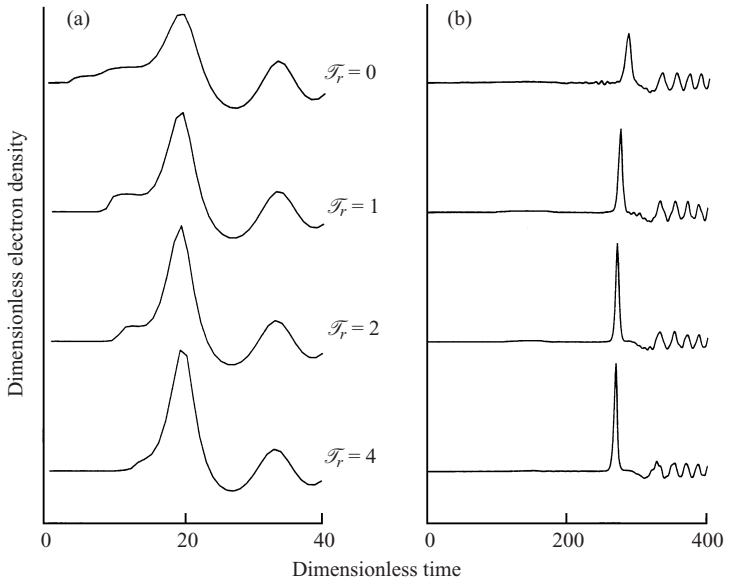

Figure 3. Evolution of the plasma close to the electrode at early times and far from the electrode at late times as the rise time of the voltage step is changed in units of $\tau_r = \mathscr{T}_r/\omega_{pi}$; $V_{\text{grid}} = 20$. (a) A voltage- and rise-time-dependent burst of ions, a burst of ions reflected from the soliton, an ion acoustic soliton, and a dispersing ion acoustic wave are detected close to the electrode at $z = 20$. (b) An ion acoustic soliton and a dispersing ion acoustic wave are detected far from the electrode at $z = 300$.

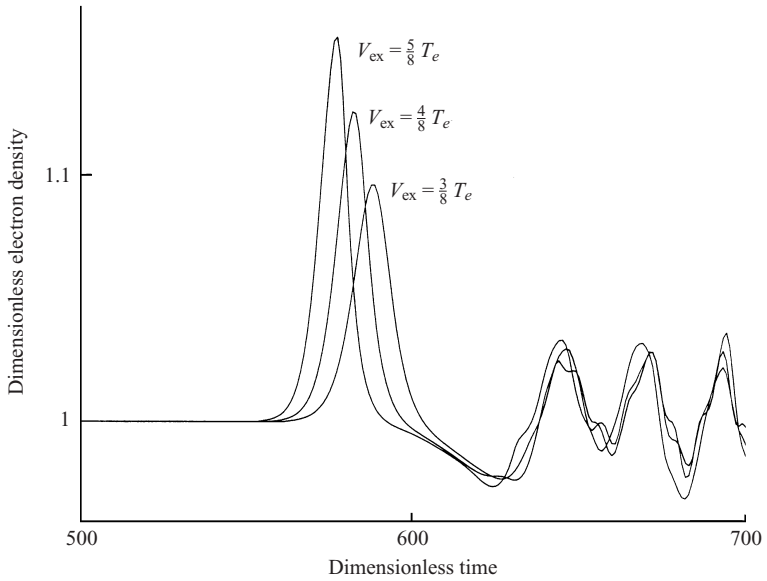

Figure 4. Propagation of an ion acoustic soliton and a dispersing ion acoustic wave far from the electrode at late times for three values of a positive step voltage. The rise time of the voltage step is zero.

https://doi.org/10.1017/S002237789800734X Published online by Cambridge University Press

Table 2. Summary of computed times of flight normalized by the linear ion acoustic velocity at three values of the excitation potential applied to the electrode.

V_{grid}	$\dfrac{\left(\frac{2eV_{\text{grid}}}{M_i}\right)^{1/2}}{\left(\frac{\kappa_B T_e}{M_i}\right)^{1/2}}$	Simulation		
		$\dfrac{\Delta n}{n}$	$\Delta T = \dfrac{600}{1+\Delta n/3n}$	ΔT
$\frac{3}{8}T_e$	0.87	0.096	581	586
$\frac{4}{8}T_e$	1.0	0.126	576	579
$\frac{5}{8}T_e$	1.12	0.157	570	574

4. Conclusions

The PIC simulation that has been performed here is in agreement with earlier laboratory experiments. They indicate that both the amplitude and the rise time of the applied voltage step are parameters that can be experimentally adjusted. These parameters control the size of the initial ion perturbation out of which one or more ion acoustic solitons evolve. Beyond some value, an increase in the excitation voltage does not increase the amplitude of the initial, self-consistent perturbation, but rather creates more burst and reflected ions. Consequently, the amplitude of the final solition is independent of the excitation amplitude for large excitation voltages. The acceleration mechanism for the reflection of ions ahead of the soliton is attributed to Fermi acceleration.

References

Alexeff, I., Jones, W. D. and Lonngren, K. E. 1968 Excitation of pseudowaves in a plasma via a grid. *Phys. Rev. Lett.* **21**, 878–881.

Amin, A., Aossey, D., Nguyen, B. T., Kim, H. S., Cooney, J. L. and Lonngren, K. E. 1993 Sheath evolution in a negative ion plasma. *Phys. Fluids* **B5**, 3813–3818.

El-Zein, Y., Amin, A., Shen, C., Yi, S., Lonngren, K. E. and Sheridan, T. E. 1996 Two dimensional sheath evolution in a negative ion plasma. *J. Appl. Phys.* **79**, 3853–3860.

Gabl, E. F. and Lonngren, K. E. 1984 On grid-launched linear and nonlinear ion acoustic waves – II. *Plasma Phys.* **26**, 799–811.

Hong, M. P. and Emmert, G. A. 1994 Two-dimensional fluid modeling of time-dependent plasma sheath. *J. Vac. Sci. Technol.* **B12**, 889–896.

Hong, M. P. and Emmert, G. A. 1995 Two dimensional fluid simulation of expanding plasma sheaths. *J. Appl. Phys.* **78**, 6967–6973.

Joyce, G., Lonngren, K. E., Alexeff, I. and Jones, W. D. 1969 Dispersion of ion acoustic waves. *Phys. Fluids* **12**, 1591–1599.

Lonngren, K. E., Aksornkitti, S., Hsuan, H. C. S., Alexeff, I. and Jones, W. D. 1970 Dispersive-like properties of accelerated ion bursts in a plasma. *J. Appl. Phys.* **41**, 821–823.

Lonngren, K. E., Chan, C. and Khazei, M. 1981 On 'Fermi-accelerated' ions from an expanding plasma sheath. *Phys. Lett.* **85A**, 33–34.

Lonngren, K. E., Khazei, M., Gabl, E. F. and Bulson, J. 1982 On grid launched linear and nonlinear ion acoustic waves. *Plasma Phys.* **24**, 1483–1489.

Sheridan, T. E. 1995 Pulsed-sheath ion dynamics in a trench. *J. Phys. D: Appl. Phys.* **28**, 1094–1098.

Sheridan, T. E. 1997 Effect of target size on dose uniformity in plasma-based ion implantation. *J. Appl. Phys.* **81**, 7153–7157.

https://doi.org/10.1017/S002237789800734X Published online by Cambridge University Press

Sheridan, T. E. and Alport, M. J. 1994 Two-dimensional model of ion dynamics during plasma source ion implantation. *Appl. Phys. Lett.* **64**, 1783–1785.

Sheridan, T. E., Yi, S. and Lonngren, K. E. 1998 On the origin of the ion acoustic soliton. *Phys. Plasmas* **5**, 3165–3170.

Widner, M., Alexeff, I., Jones, W. D. and Lonngren, K. E. 1970 Ion acoustic wave excitation and ion sheath evolution. *Phys. Fluids* **13**, 2532–2540.

Yi, S. and Lonngren, K. E. 1997 Rarefactive ion acoustic soliton excitation using a modulated high frequency sinusoidal wave in a negative ion plasma. *Phys. Plasmas* **4**, 2893–2898.

Yi, S., Bai, E. W. and Lonngren, K. E. 1997a Ion acoustic soliton excitation using a modulated high frequency sinusoidal wave. *Phys. Plasmas* **4**, 2436–2442.

Yi, S., El-Zein, Y., Lonngren, K. E. and Sheridan, T. E. 1997b Plasma sheath evolution from perturbed electrodes in a negative-ion plasma. Part 2. Experiment and PIC simulation. *J Plasma Phys.* **58**, 455–466.